



Calhoun: The NPS Institutional Archive

Faculty and Researcher Publications

Faculty and Researcher Publications Collection

1999

Variational tight-binding theory of excitons in compositionally modified semiconductor superlattices

Luban, Marshall

Superlattices and Microstructures, Vol. 25, No. 3, 1999
<http://hdl.handle.net/10945/43190>



Calhoun is a project of the Dudley Knox Library at NPS, furthering the precepts and goals of open government and government transparency. All information contained herein has been approved for release by the NPS Public Affairs Officer.

Dudley Knox Library / Naval Postgraduate School
411 Dyer Road / 1 University Circle
Monterey, California USA 93943

<http://www.nps.edu/library>



Variational tight-binding theory of excitons in compositionally modified semiconductor superlattices

MARSHALL LUBAN, JOSEPH P. REYNOLDS[†]

*Ames Laboratory and Department of Physics and Astronomy, Iowa State University,
Ames, IA 50011, U.S.A.*

JAMES H. LUSCOMBE

*Department of Physics, Naval Postgraduate School,
Monterey, CA 93943, U.S.A.*

(Received 20 August 1998)

We present results for the binding energy of an exciton formed when an electron–hole pair is photoexcited within a single, compositionally modified layer of a semiconductor superlattice, for example by adding a small percentage of In atoms to a single GaAs layer of a GaAs/AlGaAs system. Such a system could serve as the basis for spatially-selective photoexcitation, a process whereby a laser pulse would create electron–heavy-hole pairs exclusively in the modified layer. We first derive an effective one-dimensional (1D) Hamiltonian for an electron, by averaging the 3D electron–hole Hamiltonian using a one-parameter trial wavefunction, which is dependent on the in-plane relative coordinates, as well as a normalized Wannier orbital for a single hole. The exciton binding energy is then obtained by computing the lowest bound-state energy of the effective 1D electron Hamiltonian in the nearest-neighbor tight-binding approximation. As a demonstration of the effectiveness of our approach, we find that for periodic superlattices our results for the exciton binding energy are in very good agreement both with experiment and the results of other theoretical calculations.

© 1999 Academic Press

Key words: excitons, semiconductor superlattices, tight-binding model.

1. Introduction

In this article we calculate the binding energy and spatial characteristics of a bound electron–hole pair in a superlattice that has been compositionally modified in one layer, and where the hole remains confined to that layer. While the theory of excitons in periodic superlattices has reached a fairly sophisticated state,[‡] even as it continues to be refined, we are unaware of any studies in the literature concerning the character of an

[†]Present address: Department of Electrical Engineering, University of Notre Dame, South Bend, IN 46556, U.S.A.

[‡]There is a vast literature on the theory of excitons in superlattices that has been cultivated during the past decade. A useful introduction is given in the review article [1].

exciton that results in compositionally modified[†] superlattices. We will here study the example of adding In atoms in a single GaAs layer of a GaAs/AlGaAs superlattice. Apart from considerations of basic science, there may be practical benefits realizable from such a modified system. As an example, we have recently proposed [3] that a superlattice with a single In-modified layer could serve as the basis for spatially-selective photoexcitation, a process whereby a laser pulse would create electron–hole pairs exclusively in the modified layer. As discussed in Ref. [3], our calculations indicate that, by growing an InGaAs layer (<1% In) in the center of a GaAs/AlGaAs superlattice, the resulting structure will be effective for achieving spatially-selective photoexcitation. A specific benefit of this technique would be to enable the existence of substantially longer-lived Bloch oscillations than are possible with conventional superlattices[‡] by circumventing the dephasing effects of interface roughness [5]. It may also prove possible to exploit spatially-selective photoexcitation for other optoelectronic applications.

Starting from the effective-mass Hamiltonian H (see eqn (1)) for the compositionally-modified superlattice system, which includes the full three-dimensional (3D) Coulomb potential for the electron–hole pair, we arrive at a 1D effective Hamiltonian operator, H_{eff} (see eqns (11)–(13)), of the electron alone. This operator is defined by $H_{\text{eff}} \equiv \langle \Phi, h | H | \Phi, h \rangle$, where $|\Phi, h\rangle \equiv \Phi(\rho; \xi) \times |h\rangle$. The quantity $\Phi(\rho, \xi)$ is a normalized function (see eqn (5)) of the transverse (in-plane) relative electron–hole distance and one variational parameter, ξ . The second factor, $|h\rangle$, is an appropriate, normalized hole Wannier orbital, a function of the hole’s longitudinal (growth direction) coordinate z_h . The resulting operator H_{eff} is a function of the electron longitudinal coordinate z_e and the corresponding momentum operator $p_e = -i\hbar\partial/\partial z_e$. The potential energy portion, $V_{\text{eff}}(z_e; \xi)$, of H_{eff} is the sum of three terms, the conventional square-wave term for periodic superlattices, a term due to the compositional modification in a single GaAs layer, and an attractive long-ranged Coulomb term due to the photoexcited hole, which for large values of z_e , decays proportional to $1/|z_e|$. We then employ the numerical method of Ref. [6] to determine the localized energy eigenfunctions of H_{eff} , considered in the nearest-neighbor tight-binding approximation for a given value of ξ , and their corresponding energies. Of particular interest to us is $F_G(z_e; \xi)$, the localized eigenstate of H_{eff} with the lowest energy for that choice of ξ . We then vary ξ so as to determine the lowest energy, which occurs for $\xi = \xi_{\text{min}}$. The quantity $\Phi(\rho; \xi_{\text{min}}) \times |h\rangle \times F_G(z_e; \xi_{\text{min}})$ then provides an approximation for the ground-state eigenfunction of the bound exciton.

Variational approaches for computing the properties of excitons based on a separable trial function have previously proven highly robust and accurate as demonstrated, e.g. by Bastard and co-workers [1, 7] in the context of strictly periodic superlattices. To demonstrate the effectiveness of our separable trial function, we also calculate the exciton binding energy for a specific periodic superlattice (i.e. without the addition of an InGaAs layer) and compare our results with experimental data and with other theoretical calculations given in the literature [8]. In fact, our results are in very close agreement with the experimental data as well as with the best theoretical estimates that have been obtained using a variety of different trial functions.

The layout of this paper is as follows. In Section 2.1 we introduce the Hamiltonian describing the electron–hole pair as well as the form of the separable trial function used throughout this work. In Section 2.2 we arrive at the form, eqn (13), of the 1D effective electron Hamiltonian. In Section 2.3 we treat the effective electron Hamiltonian in the nearest-neighbour tight-binding approximation and we obtain the form of the localized eigenstates and their corresponding energies for a given value of ξ . In Section 3 we present our major results for two different GaAs/AlGaAs superlattice systems. One of these is the In-modified version of the periodic superlattice used extensively by Kurz *et al.* [9, 10] in their experimental studies of Bloch oscillations and the associated THz radiation. A summary and a discussion of open issues is provided in Section 4.

[†]A calculation of the binding energy of an exciton formed in a superlattice when one GaAs layer has a different width compared to all others has been given in Ref. [2].

[‡]A review of the experimental issues and compilation of the literature on the detection of Bloch oscillations and the emission of THz radiation has been given in Ref. [4].

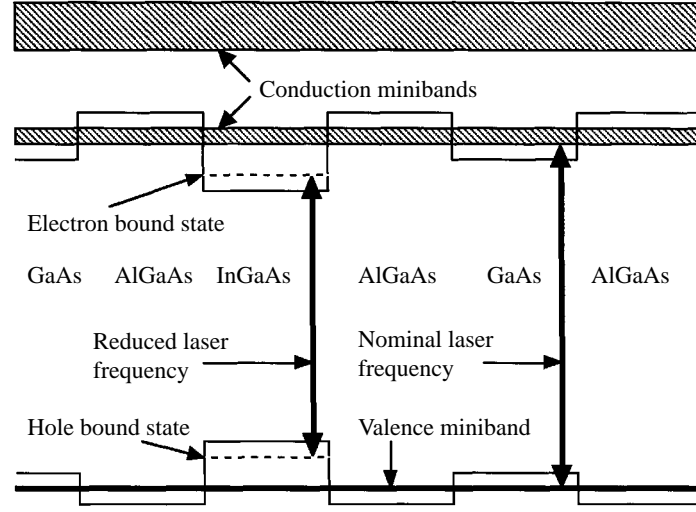


Fig. 1. Schematic diagram of an In-modified GaAs/AlGaAs superlattice. Photoexcitation of electron-hole pairs will proceed throughout the superlattice if one uses a laser pulse peaked about the 'nominal laser frequency'. However, a laser pulse peaked about the 'reduced laser frequency' and with the appropriate spectral width will photoexcite electron-hole pairs primarily only in that modified layer.

2. The method

2.1. Preliminaries

Our treatment is based on an effective-mass Hamiltonian. However, to simplify the mathematical treatment, we adopt a spatially uniform longitudinal effective mass $m_e^l(m_h^l)$ and a spatially uniform transverse effective mass $m_e^t(m_h^t)$ for conduction (heavy-hole) states. Similarly, a spatially uniform relative dielectric constant, κ , is adopted. The numerical assignments for these constants are made in terms of properly weighted averages of the effective masses and relative dielectric constants of the individual GaAs and $\text{Al}_x\text{Ga}_{1-x}\text{As}$ layers. The details of these averages and assignments are given in Section 3.1.

The addition of In atoms in a single GaAs layer reduces the band gap in that layer. Thus by using a laser pulse with an appropriately reduced excitation frequency it becomes possible to limit photoexcitation of electrons and heavy holes, primarily to the modified GaAs layer (see Fig. 1). The center of the modified layer will serve as the origin of the coordinates z_e, z_h . Because of the translational invariance of the system in the transverse direction, it is advantageous to introduce center-of-mass and relative coordinates in place of the transverse Cartesian coordinates (x_e, y_e, x_h, y_h) of the electron and hole. We may ignore the transverse center-of-mass motion, so that the Hamiltonian of interest, using SI units, is

$$H = E_g - \frac{\hbar^2}{2\mu^t} \frac{1}{\rho} \frac{\partial}{\partial \rho} \left(\rho \frac{\partial}{\partial \rho} \right) + H_e(z_e) + H_h(z_h) - \frac{e^2}{4\pi \epsilon_0 \kappa ((z_e - z_h)^2 + \rho^2)^{1/2}}, \quad (1)$$

where

$$H_e(z_e) = -\frac{\hbar^2}{2m_e^l} \frac{\partial^2}{\partial z_e^2} + V_e(z_e) + V_e^M(z_e), \quad (2)$$

$$H_h(z_h) = -\frac{\hbar^2}{2m_h^l} \frac{\partial^2}{\partial z_h^2} + V_h(z_h) + V_h^M(z_h), \quad (3)$$

and where $\rho = ((x_e - x_h)^2 + (y_e - y_h)^2)^{1/2}$. Here we choose the zero of energy to coincide with the top of the bulk GaAs valence band, E_g denotes the bandgap energy of bulk GaAs, μ^t denotes the reduced transverse mass of the electron-heavy-hole pair, $V_e(z_e)$ and $V_h(z_h)$ are the conduction and valence band minima for a periodic superlattice of period a , whereas $V_e^M(z_e)$ and $V_h^M(z_h)$ are the corresponding terms due to the modifications made in the single GaAs layer. For simplicity, throughout this work we treat the case that the In atoms are distributed uniformly in the GaAs layer, so that the functions $V_e^M(z_e)$ and $V_h^M(z_h)$ are constant in the layer and zero elsewhere. The forms of V and V^M derive from the respective band offsets and thus differ for electrons and holes; this is reflected by the subscripts e, h in (2) and (3). We suppose that the system is rotationally invariant about the growth axis, and because we restrict our attention to trial functions for the ground-state eigenfunction, we have not included a term in (1) involving the second derivative with respect to the in-plane angular coordinate.

2.2. Effective electron Hamiltonian

Our goal in this subsection is to determine the form of the effective 1D electron Hamiltonian operator $H_{\text{eff}}(z_e, -i\hbar\partial/\partial z_e; \xi)$ that follows upon adopting a separable trial function approximation based on a single, real, positive variational parameter (ξ), for the ground-state eigenfunction of (1), of the form

$$\Psi_T(\rho, z_e, z_h) = \Phi(\rho; \xi) \times |h\rangle \times F(z_e), \quad (4)$$

where

$$\Phi(\rho; \xi) = (2/\pi)^{1/2} \xi^{-1} \exp(-\rho/\xi). \quad (5)$$

In writing (5) we have adopted the normalization condition

$$\langle \Phi | \Phi \rangle \equiv 2\pi \int_0^\infty d\rho \rho |\Phi|^2 = 1. \quad (6)$$

The quantity $|h\rangle$ in (4) denotes the calculated normalized hole Wannier orbital[†] centered about the modified GaAs layer, i.e. $\langle h | h \rangle = 1$. In Section 2.3 we describe a numerical method for determining the form of $F(z_e)$ based on the single orbital, nearest-neighbor tight-binding model.

The construction of H_{eff} is achieved in two steps. We first define a 1D electron-hole Hamiltonian, based on (4)–(6), according to

$$H^I(z_e, z_h; \xi) \equiv \langle \Phi | H | \Phi \rangle. \quad (7)$$

This operator depends upon both of the longitudinal coordinates z_e and z_h , as well as the corresponding momentum operators, and the variational parameter ξ . Upon evaluating (7) one finds that

$$H^I(z_e, z_h; \xi) = E_g + \frac{\hbar^2}{2\mu^t \xi^2} + H_e(z_e) + H_h(z_h) + V^c(z_e - z_h; \xi), \quad (8)$$

where

$$V^c(z; \xi) \equiv -\langle \Phi | \frac{e^2}{4\pi \epsilon_0 \kappa (z^2 + \rho^2)^{1/2}} | \Phi \rangle = V^c(0; \xi) u(Z), \quad (9)$$

$$V^c(0; \xi) = -\left(\frac{e^2}{4\pi \epsilon_0 \kappa} \right) \left(\frac{2}{\xi} \right), \quad (10)$$

and

$$u(Z) \equiv Z \{-1 + (\pi/2)[H_1(Z) - Y_1(Z)]\}. \quad (11)$$

[†]For practical calculations, the normalized hole Wannier orbital is obtained by numerical integration methods from the hole Bloch eigenstates which we have derived for the periodic version of each superlattice system considered in Section 3.

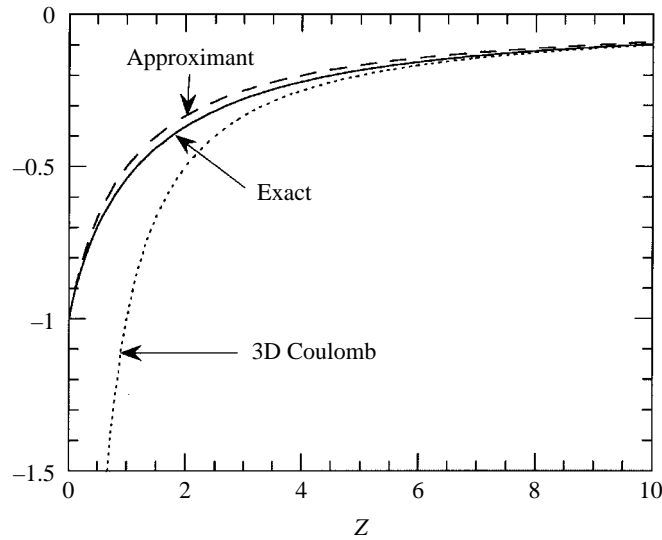


Fig. 2. The full curve provides the function $u(Z)$ given by eqn (11). In the text we have approximated this function by the rational approximant $1/(1 + Z)$ shown as the long-dash curve. The short-dash curve gives the 3D Coulomb expression $1/Z$.

The quantity $Z = 2|z|/\xi$ is positive whatever the sign of z , H_1 is a Struve function, and Y_1 denotes a standard Neumann function. Using eqns (9.1.11), (12.1.5), and (12.1.31) from [11] one finds that $u(0) = 1$, whereas for $Z \gg 1$ one has $u(Z) \rightarrow 1/Z$ and thus $V^c(z; \xi) \rightarrow V^c(0; \xi)/Z = -e^2/(4\pi\epsilon_0\kappa|z|)$. In Fig. 2 the full curve is a plot of $u(Z)$ for $0 \leq Z \leq 10$. The simple rational approximant $1/(1 + Z)$, shown as the long-dash curve in Fig. 2, not only incorporates the correct limiting properties of $u(Z)$ for $Z = 0$ and for $Z \gg 1$ but it also provides a good approximation for all Z . Finally, the short-dash curve in Fig. 2 is a plot of the '3D Coulomb potential' defined as $-e^2/(4\pi\epsilon_0\kappa|z|)$ for all z . In short, for any nonzero given value of ξ the effective 1D Coulomb potential (9) is smaller in magnitude than the 3D Coulomb form, yet rapidly approaches the latter from above for $Z \gg 1$. Note that V^c , as given by (9), vanishes in the large ξ limit for any fixed value of z .

In the following, rather than work with the cumbersome exact expression, (11), for $u(Z)$, we adopt the very convenient, reasonably accurate rational approximant $1/(1 + Z)$ so as to arrive at the following approximate expression for the longitudinal 1D electron-hole Hamiltonian operator,

$$H^l(z_e, z_h; \xi) = E_g + \frac{\hbar^2}{2\mu^l \xi^2} + H_e(z_e) + H_h(z_h) - \left(\frac{e^2}{4\pi\epsilon_0\kappa} \right) \left(\frac{2}{\xi} \right) \frac{1}{1 + (2|z_e - z_h|/\xi)}. \quad (12)$$

The last term of (12) provides the coupling of the longitudinal coordinates z_e and z_h .

We now embark on the second leg of our procedure, that of decoupling the electron and hole coordinates, so as to arrive at an expression that depends only on the electron coordinates, by forming the scalar product $\langle h | H^l | h \rangle$. The resulting 1D Hamiltonian, to be denoted by H_{eff} , depends on z_e and the variational parameter ξ , and it is given by

$$H_{\text{eff}}(z_e; \xi) = E_g + \frac{\hbar^2}{2\mu^l \xi^2} + \langle h | H_h | h \rangle - \frac{\hbar^2}{2m_e^l} \frac{\partial^2}{\partial z_e^2} + V_{\text{eff}}(z_e; \xi), \quad (13)$$

where

$$V_{\text{eff}}(z_e; \xi) = V_e(z_e) + V_e^A(z_e; \xi), \quad (14)$$

and $V_e^A(z_e; \xi)$ denotes the total aperiodic portion of the electron potential $V_{\text{eff}}(z_e; \xi)$. It is defined by

$$V_e^A(z_e; \xi) \equiv V_e^M(z_e) + V_e^c(z_e; \xi), \quad (15)$$

where (see footnote, p. 496)

$$V_e^c(z_e; \xi) = -\left(\frac{e^2}{4\pi\epsilon_0\kappa}\right)\left(\frac{2}{\xi}\right)\langle h|\frac{1}{1+(2|z_e - z_h|/\xi)}|h\rangle \quad (16)$$

is the effective Coulomb potential energy of the electron due to its interaction with the hole, and it is a function of the variational range parameter ξ . The term $\langle h|H_h|h\rangle$ in (13) is a constant independent of both ξ and the electron coordinate z_e .

Note that if $z_e = 0$ the integral (16) remains finite. If $|z_e \pm w/2|/\xi \gg 1$ we can replace the denominator in (16) by $1 + (2|z_e|/\xi)$ and thus we have, to leading order,

$$V_e^c(z_e; \xi) \approx -\frac{e^2}{4\pi\epsilon_0\kappa} \frac{1}{(\xi/2) + |z_e|}.$$

In short, the Coulomb-based portion, $V_e^c(z_e; \xi)$, is a long-range potential, exhibiting a $1/|z_e|$ decay for large distances whereas it remains finite for $z_e \rightarrow 0$. By contrast, the short-range function $V_e^M(z_e)$ is nonzero only in the central GaAs layer, due to the addition of In atoms exclusively in that layer.

2.3. Tight-binding model

In this subsection we briefly discuss the method we use for computing the normalized, localized eigenstates of the 1D effective Hamiltonian of (13) when we employ a single-orbital, nearest-neighbor tight-binding approximation. We find that the nearest-neighbor approximation is satisfactory for the specific superlattices considered in Section 3. The basis states $|n\rangle = \omega(z_e - na)$, with $\langle n|n'\rangle = \delta_{n,n'}$, utilize a single electron Wannier orbital,[†] $\omega(z_e)$, which we derive from the Bloch states associated with the lowest electron energy band of the unmodified (no In atoms) superlattice. In the tight-binding approximation an energy eigenfunction is written as

$$F(z_e) = \sum_{n=-\infty}^{\infty} y_n \omega(z_e - na). \quad (17)$$

In particular, we are employing a model of an infinite superlattice. The expansion coefficients y_n satisfy the three-term recurrence formula

$$y_{n+1} + y_{n-1} = b_n y_n, \quad (18)$$

where

$$b_n = (E - \epsilon_n)/V_H, \quad (19)$$

E is the energy eigenvalue, $\epsilon_n = \langle n|H_{\text{eff}}(z_e; \xi)|n\rangle$ will be referred to as the site energy, and $V_H = \langle 0|H_{\text{eff}} - V_e^A|1\rangle$ is the hopping matrix element. Note that the overlap integrals $\langle n|V_e^A|n+1\rangle$ have been discarded.

We first summarize some of the major features of the mathematical analysis and numerical method of [6] for solving the infinite system of recurrence eqns (18). We first remark that (18) possesses two linearly independent solutions for any choice of E . Of central importance is an auxiliary function (see eqn (9) of [6]) which is a function of the energy parameter E and whose zeros provide the set of all energies for which (18) possesses localized solutions, i.e. solutions which decrease to zero for *both* of $n \rightarrow \pm\infty$. In particular, for localized solutions the normalization sum $\sum_n |y_n|^2$ is convergent when the sum over n extends from $-\infty$ to

[†]The electron Wannier function $\omega(z_e)$ is constructed by applying numerical integration methods to analytical expressions we have derived for the Bloch functions of the periodic version of the superlattice.

∞ . The zeros of the auxiliary function occur only for a discrete spectrum of energy eigenvalues. For all other choices of E the pair of linearly independent solutions of (18) will necessarily diverge for either or both of $n \rightarrow \pm\infty$. Between any pair of successive zeros the auxiliary function possesses a simple pole. In practice, the numerical method of Ref. [6] can be used to provide the form of the localized eigenstates and their energies to arbitrarily high accuracy. The major feature of that method is that it employs a backward recurrence scheme and thereby completely overcomes the numerical instability originating in the growing solution of (18) which inevitably accompanies a localized solution. Numerical values of the auxiliary function are computed for a large set of values of E in any energy interval of interest. In general, care must be taken to select a sufficiently fine mesh so as not to overlook a zero. This process is aided somewhat by the zero-pole-zero characteristics of the auxiliary function.

There are also energy intervals in which the auxiliary function fails to exist, and these intervals correspond to energy bands of extended states [6]. An extended state is such that $|y_n|$ remains finite (but does not vanish) for both of $n \rightarrow \pm\infty$, and yet the above normalization sum diverges as the sum over n extends from $-\infty$ to ∞ .

We remark that for the superlattices considered in Section 3 the calculation of the localized exciton eigenstates and their energies is especially easy, since these can only occur for energies below the bulk GaAs conduction band minimum. We do, in fact, find a sequence of discrete energies associated with localized solutions. The spacing of successive localized energies rapidly decreases as we proceed to higher energy, i.e. the eigenvalue spectrum has the character of an exciton spectrum. The upper endpoint of this spectrum appears to coincide with the bottom of the bulk GaAs conduction band minimum. For a wide energy interval commencing with this endpoint the auxiliary function does not exist, and, as remarked above, this is the signal [6] that in this energy interval the solutions of (18) are extended states. The spatial range of the localized solutions increases rapidly with increasing energy.

3. Numerical results

3.1. Parameter choices

As stated at the outset of Section 2, we have simplified our calculations by choosing uniform values for each of the electron and hole effective masses, m_e^l , m_e^t , m_h^l , and m_h^t as well as the relative dielectric constant κ . For the individual bulk GaAs and $\text{Al}_x\text{Ga}_{1-x}\text{As}$ layers we use the formulas $m_e^l = m_e^t = (0.067 + 0.083x)m_e$ for the electron effective masses, as well as $m_h^l = (0.38 + 0.31x)m_e$, and $m_h^t = 0.18m_e$ for the hole effective masses. Here m_e denotes the free electron mass. The above formulas are to be found in the literature, although they are by no means unique. Our assignment for $m_e^t = m_e^l$ is taken as the average of this quantity using the square of the electron Wannier function as the weighting function. With this assignment, the reduced transverse mass μ^t is then taken as $1/\mu^t = 1/m_h^t + 1/m_e^t$.

For the individual bulk GaAs and $\text{Al}_x\text{Ga}_{1-x}\text{As}$ layers we used the formula $\kappa = 12.53 - 2.47x$, which provides linear interpolation between values of κ for GaAs, (12.53), and AlAs, (10.06), given in Ref. [13]. In the following we relate to superlattices studied at low temperatures and thus we prefer this formula over a different linear interpolation formula in the literature, $\kappa = 13.18 - 3.12x$, that utilizes a measured value of κ obtained for a room-temperature sample of GaAs. As in the case of the electron effective mass, a uniform value of the relative dielectric constant was assigned by averaging the interpolation formula for κ using the square of the electron Wannier function as the weighting function.

3.2. Superlattice I

The first system that we consider is a GaAs/ $\text{Al}_{0.3}\text{Ga}_{0.7}\text{As}$ superlattice, with GaAs and AlGaAs layers of width 9.7 nm and 1.7 nm, respectively. We are particularly interested in this choice of parameters as they

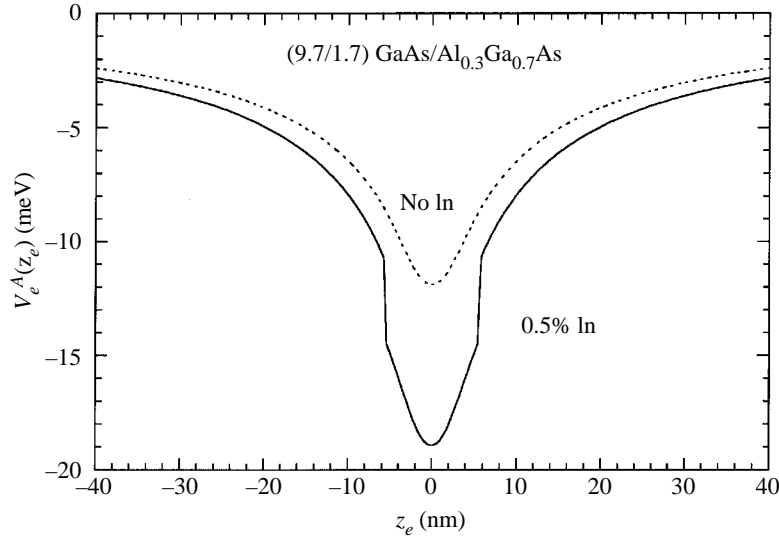


Fig. 3. The aperiodic portion, $V_e^A(z_e; \xi)$, of the effective 1D electron potential $V_{\text{eff}}(z_e; \xi)$ (see (14)–(16)) for two GaAs/Al_{0.3}Ga_{0.7}As superlattices (GaAs/Al_{0.3}Ga_{0.7}As layer widths are 9.7 and 1.7 nm, respectively). For one of these superlattice In atoms have been added to the central GaAs layer (its center corresponds to $z_e = 0$) with a concentration of 0.5%, whereas for the second superlattice no In atoms have been added.

correspond to the superlattice that was studied in the experiments on Bloch oscillations described in Refs. [9] and [10]. We find through detailed calculations that the ratio $\langle 0 | H_{\text{eff}} - V_e^A | 2 \rangle / \langle 0 | H_{\text{eff}} - V_e^A | 1 \rangle$ is very nearly 0.1. Also, we find that off-diagonal matrix elements $\langle 0 | V_e^A | n \rangle$, ($n \neq 0$) are less than $0.02 |\langle 0 | V_e^A | 0 \rangle|$ in all cases. We believe that these results are such as to justify the use of the nearest-neighbor tight-binding approximation for this superlattice.

The computed values of the aperiodic portion $V_e^A(z_e; \xi)$ of the effective electron potential energy are shown in Fig. 3. These results were obtained for the choices 0, 0.5% as the percentage additions of In atoms to the central GaAs layer. Each of the curves shown are for the minimizing values of ξ which we found to be 16.057 nm (no In) and 13.950 nm (0.5% In). The long-range character of the electron–hole Coulomb interaction is evident in both cases. It should be noted that the corresponding drop in the electron conduction band minimum in the In-modified layer, compared to that of bulk GaAs[†] is 3.458 meV.

The calculated forms of the exciton ground-state eigenfunction $F_G(z_e)$ are shown in Fig. 4 for these two choices of In. As expected the eigenfunction does not change sign, has even parity, and displays a sequence of local maxima, one for each GaAs layer, that decrease in value as one proceeds away from the center of the superlattice. The forms shown utilize (17) in conjunction with the computed values of y_n . In the absence of In we find that the exciton binding energy (measured from the bulk GaAs conduction band minimum) is 4.0111 meV. With 0.5% In, the binding energy is increased by 3.098 meV to become 7.1092 meV. These quantitative effects are in accord with the qualitative expectation that if we compare a given GaAs/AlGaAs

[†] We have determined the drop in the conduction band minimum, ΔE_c , for the In_xGa_{1-x}As layer, relative to that for GaAs according to the formula $\Delta E_c = -0.69x$ (eV). This is obtained from InGaAs bandgap data given by H. C. Casey and M. B. Panish, *Heterostructure Lasers* (Academic, New York, 1978) and the assumption of the ‘65/35’ rule for the band offsets. Being unaware of any band-offset data for the AlGaAs/InGaAs heterojunction, we assume that the ‘transitivity’ rule (which has been verified experimentally and theoretically for a number of material systems) holds between the AlGaAs/GaAs and GaAs/InGaAs heterojunctions. We note, however, that experimental determinations of the band offset for the InGaAs/GaAs heterojunction are quite varied; see the review article [12].

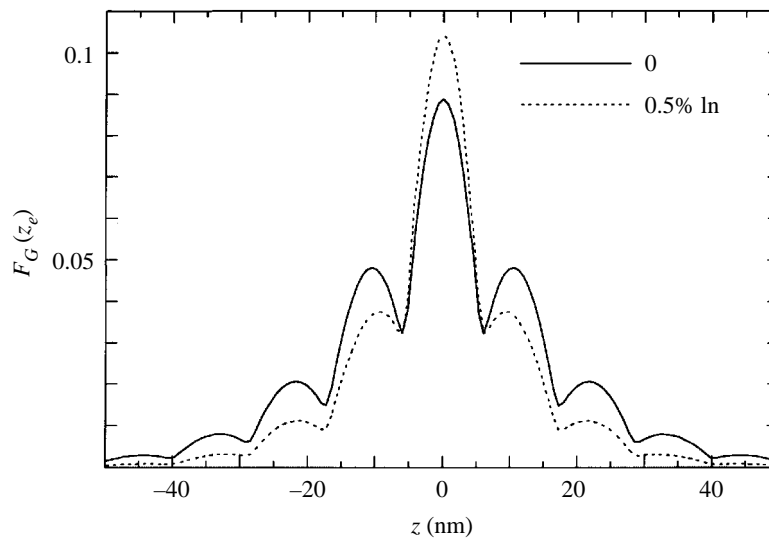


Fig. 4. The portion $F_G(z_e)$ of the exciton ground-state eigenfunction, for the two GaAs/Al_{0.3}Ga_{0.7}As superlattices considered in Fig. 3. With the addition of In atoms to the central GaAs layer the local conduction band minimum is reduced by 3.458 meV, and this gives rise to an exciton ground state that is more localized than in the superlattice without the added In atoms.

superlattice with that having an In-modified GaAs layer, as a result of the decrease in the local conduction band minimum relative to that of GaAs, the exciton ground state will have an increased binding energy and enhanced localization.

3.3. Superlattice II

The exciton binding energy has been measured [7] by optical methods for GaAs/Al_{0.3}Ga_{0.7}As superlattices which feature equal well and barrier thicknesses. The experimental values and their corresponding error bars, given in Ref. [7], are reproduced in Fig. 5. The full curve gives our theoretical prediction as a function of superlattice period, a , when we use the nearest-neighbor tight-binding approximation and vary the variational parameter ξ so as to obtain the lowest possible ground-state energy (largest binding energy) for that choice of a . The corresponding (dashes) curve giving the minimizing value, ξ_{\min} , as a function of a is also shown in Fig. 5. The agreement between experiment and our theory is very satisfactory. It should be noted that the authors of Ref. [7] also provided the results of a variational calculation which are in satisfactory agreement with the experimental data. Other theoretical calculations giving comparable results can be found in the articles of Ref. [8]. We remark that for values of a which are less than 6 nm the use of the nearest-neighbor tight-binding model is inappropriate, for in that range we find that the ratio $\langle 0|H_{\text{eff}} - V_e^A|2\rangle / \langle 0|H_{\text{eff}} - V_e^A|1\rangle$ exceeds 0.1.

4. Summary and discussion

In this article we have developed and applied a hybrid variational tight-binding theory so as to calculate the properties of an exciton in a compositionally modified semiconductor superlattice. In our approach, we adopt a separable ground-state wavefunction that includes a single-parameter trial function of the lateral coordinates, a hole Wannier orbital, as well as a numerically calculated localized eigenstate in the growth direction of the superlattice. A key feature of our method, as part of the minimization procedure, is to derive an analytic,

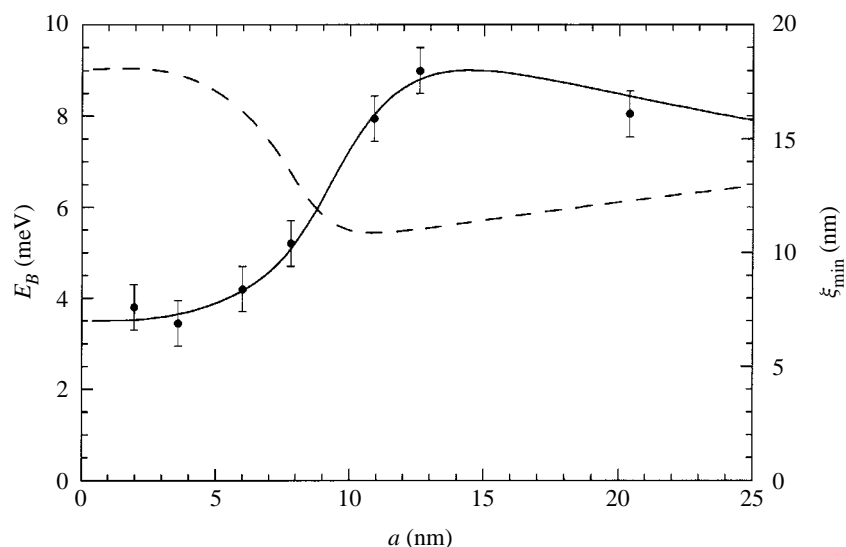


Fig. 5. Results of the present theoretical calculations for the exciton binding energy (full curve), E_B , and ξ_{\min} (dashes), the minimizing value of the variational parameter ξ , for the sequence of GaAs/Al_{0.3}Ga_{0.7}As superlattices with barrier thickness equal to well thickness as functions of superlattice period a . The data points for E_B have been reproduced from Ref. [7].

effective 1D Hamiltonian of the electron coordinate only. In particular, the variational parameter appears in the effective electron potential, as part of a modified, long-range Coulomb potential. We then solve, for a given value of the variational parameter, the remaining quantum-mechanical problem of an electron in this effective potential using a high-accuracy numerical method, after adopting the nearest-neighbor tight-binding approximation. As a check on the accuracy of our approach, we have also calculated the binding energy of excitons in purely periodic superlattices, and have found excellent agreement with both experimental data and previous theoretical calculations of the binding energy.

As stated in the Introduction, apart from its intrinsic interest, our purpose in examining the properties of excitons in a compositionally modified superlattice relates to the idea of *selective photoexcitation*, the ability to photoexcite electrons in specific layers of semiconductor heterostructures. We have proposed elsewhere [3] that selective photoexcitation in an otherwise periodic superlattice should lead to substantially longer-lived Bloch oscillations than have been attained to date. At an intuitive level, it seems plausible that lowering the bandgap of one or more selected layers should enable the occurrence of selective photoexcitation in those layers. On the other hand, the exciton so created also gives rise to a significant, long-ranged modified Coulomb potential. Thus, the ability to accurately predict the exciton binding energy and the form of the ground-state eigenfunction in such a compositionally modified system becomes of crucial importance in order to provide realistic parameters such that selective photoexcitation can in fact be achieved. To answer this need has been the task of the present work.

References

- [1] G. Bastard, J. A. Brum, and R. Ferreira, *Solid State Physics*, edited by H. Ehrenreich and D. Turnbull (Academic, New York, 1991), Vol. 44, Sec. VII. For a recent comprehensive work see N. Linder, *Phys. Rev. B* **55**, 13 664 (1997) and references cited.
- [2] S. M. Cao, M. Willander, E. W. Ivchenko, A. I. Nesvizhskii, and A. A. Toropov, *Superlattices and Microstructures* **17**, 97 (1995).

- [3] J. P. Reynolds, M. Luban, and J. H. Luscombe, (unpublished).
- [4] H. A. Kurz, H. G. Roskos, T. Dekorsy, and K. Köhler, *Phil. Trans. R. Soc. Lond.* **A354**, 2295 (1996).
- [5] J. P. Reynolds and M. Luban, *Phys. Rev.* **B54**, R14 301 (1996).
- [6] M. Luban and J. H. Luscombe, *Phys. Rev.* **35**, 9045 (1987).
- [7] A. Chomette, B. Lambert, B. Deveaud, F. Clerot, A. Regreny, and G. Bastard, *Europhys. Lett.* **4**, 461 (1987); J. A. Brum and G. Bastard, *J. Phys.* **C18**, L789 (1985).
- [8] P. M. Young, H. Ehrenreich, P. M. Hui, and N. F. Johnson, *J. Appl. Phys.* **74**, 7369 (1993); M. M. Dignam and J. E. Sipe, *Phys. Rev.* **B41**, 2865 (1990).
- [9] T. Dekorsy, P. Leisching, K. Köhler, and H. Kurz, *Phys. Rev.* **B50**, 8106 (1994).
- [10] C. Waschke, H. G. Roskos, R. Schwedler, K. Leo, and H. Kurz, *Phys. Rev. Lett.* **70**, 3319 (1993).
- [11] M. Abramowitz and I. A. Stegun, *Handbook of Mathematical Functions*, (Dover Press, New York, 1966).
- [12] E. T. Yu, J. O. McCaldin, and T. C. McGill, *Solid State Physics*, edited by H. Ehrenreich and F. Spaepen (Academic, New York, 1992), Vol. 46, pp. 1–146.
- [13] *Landolt–Börnstein, Numerical Data and Functional Relationships in Science and Technology*, edited by O. Madelung (Springer, Berlin, 1982), Ser. III, Vol. 17a, pp. 167 and 243.